



Published in final edited form as:

Mult Scler. 2014 March ; 20(3): 349–355. doi:10.1177/1352458513495935.

Gradient echo MRI correlates with clinical measures and allows visualization of veins within MS lesions

Jie Luo, PhD¹, Dmitriy A. Yablonskiy, PhD¹, Charles F. Hildebolt, DDS, PhD¹, Samantha Lancia, MS², and Anne H. Cross, MD²

¹Department of Radiology, Washington University, St. Louis MO, 63130, USA

²Department of Neurology, Washington University, St. Louis MO, 63130, USA

Abstract

Background—Conventional MRI methods do not quantify the severity of MS white matter lesions or measure pathology within normal-appearing white matter (NAWM).

Objective—Gradient Echo Plural Contrast Imaging (GEPCI), a fast MRI technique producing inherently co-registered images for qualitative and quantitative assessment of MS, was used to 1) correlate with disability; 2) distinguish clinical MS subtypes; 3) determine prevalence of veins co-localized within lesions in WM.

Methods—Thirty subjects representing RRMS, SPMS and PPMS subtypes were scanned with clinical and GEPCI protocols. Standard measures of physical disability and cognition were correlated with MR metrics. Lesions with central veins were counted for RRMS subjects.

Results—Tissue damage load (TDL-GEPCI) and lesion load (LL-GEPCI) derived with GEPCI correlated better with MS functional composite (MSFC) measures and most other neurologic measures than lesion load derived with FLAIR (LL-FLAIR). GEPCI correctly classified clinical subtypes in 70% subjects. A central vein could be identified in 76% of WM lesions in RRMS subjects on GEPCI T2*-SWI images.

Conclusion—GEPCI lesion metrics correlated better with neurologic disability than lesion load derived using FLAIR imaging, and showed promise in classifying clinical subtypes of MS. These improvements are likely attributable to the ability of GEPCI to quantify tissue damage.

Keywords

Multiple Sclerosis; quantitative MRI; CNS white matter; MS clinical subtypes; perivascular cuffs

Correspondence: Anne H. Cross, MD, crossa@neuro.wustl.edu, Neurology, Campus Box 8111, 600 South Euclid Ave., St. Louis, MO 63110, (314) 747-0405 office.;

Declaration of Conflicting Interests

Dr. Cross has received research and clinical trial funding from the NIH, the U.S. Dept. of Defense, National MS Society USA, Consortium of Multiple Sclerosis Centers, the Barnes-Jewish Hospital Foundation, Hoffman-La Roche, and Sanofi, and honoraria or consulting fees from Hoffman-La Roche, Sanofi, Novartis, GlaxoSmithKline, Bayer Healthcare, Biogen Idec, Genzyme, Questcor, and Teva Neuroscience.

Introduction

Magnetic resonance imaging (MRI) plays a key role in diagnosis of multiple sclerosis (MS). Numerous MRI techniques have been used in MS over the years, with conventional T1-weighted (T1W), T2-weighted (T2W) and Fluid Attenuated Inversion Recovery (FLAIR) imaging techniques the most widely used in clinic. However, results based on T2W lesions do not correlate well with MS disability.¹ Lack of correlation between clinical findings and standard imaging is especially noted in the progressive clinical subtypes,^{2, 3} the subtypes where effective treatments are most needed. This so-called “clinic-radiological paradox,” has been attributed to multiple factors, including the complexity and heterogeneity of the underlying tissue damage in MS, differing effects on function caused by different lesion locations, as well as to variable degrees of neural plasticity among patients.⁴ Another reason for the paradox might be that image contrast in standard “weighted” spin-echo sequences depends not only on the tissue-damage-affected MR relaxation time constants of the tissue but also on the parameters of the pulse sequence. This non-biological factor may lead to a weaker correlation between MR measurements and disability measurements. The first and last of these shortcomings can be overcome by using measures of tissue T2 and T1 relaxation times instead of using T2- and T1-weighted images.^{5, 6} Notably, pathology within autopsied MS brain tissue showed good correlation with T1 and T2 relaxation time constants, invoking the potential for using these methods to quantitate MS tissue damage.⁶ However, the methods proposed in these studies^{5, 6} are clinically impractical because of the long scanning times needed for accurate measurements. Thus, practical quantitative imaging is needed, especially for the timely evaluation of new therapies.^{7, 8}

Gradient Echo Plural Contrast Imaging (GEPCI) developed in our laboratory is a post processing technique based on a multi-echo gradient echo sequence. It provides basic contrasts such as T1W images and quantitative T2* maps and also offers additional images that differentiate gray from white matter, and reveal venous structures.⁹ Importantly, GEPCI method for measuring white matter damage based on the T2* maps is quantitative.¹⁰ In this study, we compared cerebral white matter GEPCI quantitative scores with traditional lesion load assessments for correlations with clinical test scores, finding GEPCI scores to correlate with clinical test results consistently better than traditional T2W lesion load (LL). GEPCI also showed promise for differentiating clinical MS subtypes. GEPCI images are inherently co-registered, enabling the precise determination of relationships between structures revealed by different contrasts. Thus, we used GEPCI to detect co-localization of MS lesions and veins in CNS white matter, a property that may aid in better understanding lesion pathogenesis.¹¹

Materials and methods

Standard protocol approvals and patient consent

This study was approved by the local Human Research Protection Office/Institutional Review Board. All subjects provided written informed consent.

Subjects—Ten subjects per group representing RRMS, SPMS, and PPMS clinical subtypes were recruited from patients attending The John L. Trotter MS Center. Progressive

relapsing MS patients were not included, as we have very few at our clinic. RRMS subjects had been followed for a minimum of one year, and the PPMS and SPMS subjects had been followed for at least four or five years, respectively, to confirm the clinical subtype. Subjects were recruited such that EDSS scores were overlapping between groups as much as possible.

MRI protocol—Magnetic resonance (MR) data were acquired on a 3T MR Trio scanner (Siemens, Erlangen, Germany) using a 12-channel phased-array head transmit/receive coil. Subjects were instructed to minimize movement during the scan.

Proton density weighted and T2 weighted images were obtained with one acquisition by turbo spin echo sequence (TSE), TR = 6800 ms, TE1 = 12 ms, TE2 = 96 ms, flip angle 150°, turbo factor = 7, echo trains per segment = 28. Standard FLAIR images were acquired by TSE sequence: TR = 10 s, TI = 2600 ms, TE = 82 ms, turbo factor = 13, echo trains per segment = 15. T1 weighted images were acquired using spin echo (SE) sequence: TR = 600 ms, TE = 12 ms, FA1 = 90°, FA2 = 180°. All these standard images had resolution 1.3×0.9×3.0 mm³ with total acquisition time 15.8 minutes.

GEPCI data were obtained using a 3D version of the multi gradient echo sequence with a resolution of 1×1×3 mm³, field of view of 256 × 192 × 120 mm³, and 11 gradient echoes (minTE=4 ms; delta-TE=4 ms; TR=50 ms; bandwidth= 510 Hz/Pixel; FA=30°) was used, with a total acquisition time of 6.4 minutes.

Clinical tests—On the day of imaging, EDSS (Expanded Disability Status Scale) was performed by a neurostatus-certified neurologist.¹² Multiple Sclerosis Functional Composite (MSFC 2'' and MSFC 3'') comprised of timed 25-foot walk, 9-hole peg test and 3-second and 2-second paced auditory serial addition task (PASAT) was performed. Symbol Digital Modality Test (SDMT) a cognitive measure sensitive to deficits typically seen in MS patients, was also performed.¹³

MRI data analysis—Image reconstruction and post-processing of GEPCI data were performed using a standard PC computer and Matlab software (Math-Works Inc.).

After treating multi-channel data as described in ⁹, signal was expressed as

$$S(T E_n) = S_0 \cdot e^{-R2^* \cdot T E_n} \cdot e^{i2\pi f \cdot T E_n} \quad [1]$$

After fitting this model to data for each imaging voxel, T1weighted (S_0) images and maps of $R2^*$, $T2^*$ ($=1/R2^*$) and frequency (f) were generated.

GEPCI scores were then generated as reported previously.¹⁰ The first step was the design of the masks that contain the cerebral white matter volume, including both normal-appearing white matter (NAWM) and lesion areas. On T1W-GEPCI images, these masks were manually drawn using home-built Matlab programs. All gray matter structures (cortical and deep) were excluded as well as areas near the auditory canals and sinuses which are susceptible to field inhomogeneities. Masks were applied on GEPCI- $R2^*$ maps. Then $R2^*$ histograms of the voxels inside the mask volume were generated using a bin width of 0.3 s⁻¹

ranging from 0 s^{-1} up to 30 s^{-1} . For normal control subjects, these histograms have a quasi-Gaussian shape. For subjects with MS, there is typically a similar large peak with a quasi-Gaussian shape (corresponding to NAWM) and a non-Gaussian tail resulting from MS lesions with lower $R2^*$.

Characteristics of the $R2^*$ distribution, such as center position of the quasi-Gaussian shape $R2^*_{(c)}$ and full width at half maximum of the distribution $R2^*_{(w)}$ are recorded as part of GEPCI outcome. To separate “normal appearing white matter” from MS lesions we use $R2^* = R2^*_{(c)} - 1.96 R2^*_{(w)}$, as a threshold, and assign total volume of voxels that have lower $R2^*$ as lesion load (LL-GEPCI). Tissue damage score (TDS) is then defined for each lesion voxel:

$$TDS = \frac{R2^*_{(c)} - R2^*}{R2^*_{(c)}}, \quad [2]$$

tissue damage load (TDL-GEPCI) is subsequently calculated by

$$TDL = V \cdot \sum_{i=1:N} TDS_i, \quad [3]$$

where V is the voxel volume (mm^3), and N is total number of lesion voxels.

FLAIR based lesion load (LL-FLAIR) was determined by manually drawing ROIs on FLAIR images with a home-built semi-automatic Matlab program in which a voxel within a lesion is identified by the examiner. The program automatically evaluates whether neighboring voxels also belong to this lesion by calculating signal differences between them and includes more voxels as appropriate. Afterwards, the examiner reviewed the ROIs for accuracy.

The images with derived contrasts FST2*, T1f, SWI, and T2*-SWI were also obtained using the procedure described in ⁹, note that zero filling in k-space was applied to enhance effective resolution of the images. Numbers of lesions which were associated with a central vein were counted in RRMS subjects.

Statistical analysis—Analyses were performed with JMP[®] Statistical Software Release 10.0.0 (SAS Institute, Inc., Cary, NC).¹⁴ Since our subject group numbered thirty, not unexpectedly all parameters were non-normally distributed (Shapiro-Wilk W test, $p < 0.05$), and thus non-parametric Spearman ρ was used to examine cross correlations between clinical measurements and traditional imaging measurements and GEPCI scores. Alpha (the criterion for significance) was set at < 0.05 .

The ‘Decision Tree’ method in the partition platform in JMP[®] was used to differentiate MS subtypes. The goal was to use a series (as few as possible) of logical if-then conditions (tree nodes) to classify cases. The “predictor variables” were assigned to be either a set of GEPCI metrics (TDL, LL, MTDS, $R2^*_{(w)}$, $R2^*_{(c)}$, $R2^*_{(w)}/R2^*_{(c)}$) or a set of clinical test scores (PASAT 2” and 3”, 25’ walk, 9-HPT, MSFC 2” and 3”, EDSS, MSSS) to predict “dependent variables” (RRMS, PPMS and SPMS).

Results

RRMS, SPMS, and PPMS clinical subtypes had EDSS score ranges of 1.5-6.5, 4.0-6.5, and 3.5-8.0, respectively (Demographics summarized in Table 1). The RRMS group was younger and with shorter disease duration than the other two groups. Since the SPMS subtype by definition is at a later stage than RRMS, it was not unexpected that disease duration of the SPMS subjects was longer than the RRMS subjects. The PPMS group demonstrated the most aggressive disease, as the median EDSS score was similar to that of SPMS but with shorter disease duration (Table 1). Characteristics of imaging metrics (GEPCI and FLAIR) for each clinical group are described in supplementary Table S1.

Correlations between Clinical and Radiological measurement

Several parameters determined using GEPCI correlated with clinical measures (Table 2). TDL accounts for both lesion volume and severity of tissue damage based on T2* relaxation times. In keeping with our initial hypothesis, TDL provided the strongest correlations with clinical measures. LL-GEPCI, the GEPCI-determined equivalent to the standard LL determined by qualitative FLAIR (LL-FLAIR) correlated with MSFC 3", MSFC 2" and all of the individual components of MSFC except PASAT 3" and with SDMT. Moreover, LL-GEPCI provided stronger correlations than LL-FLAIR in all cases except 9HPT. For PASAT 2" version, only GEPCI scores, but not LL-FLAIR, correlated with the scores. Lack of correlations of any of the imaging scores with PASAT 3" was likely due to the insensitivity of the easier PASAT 3" to differentiate mild abnormalities in our patients, as PASAT 3" scores were 59/60 or a perfect 60/60 in more than 25% (8/30) of our subjects.

Differentiating MS subtypes based on GEPCI or Clinical evaluations

Another goal of this study was to determine if GEPCI would discriminate among clinical MS subtypes. Ten subjects per group representing the RRMS, SPMS, and PPMS subtypes were studied. The patients were chosen to span a range of EDSS disability levels, attempting to overlap EDSS scores among groups. Using all GEPCI parameters as potential factors to predict MS subtypes, decision tree methodology correctly identified all ten SPMS subjects, seven of ten RRMS, but only four of ten PPMS subjects. Overall, 70% of the thirty subjects were assigned the correct clinical subtype, based on GEPCI. In contrast, 80% of the thirty subjects were correctly identified using the clinical measurements.

GEPCI contrasts allowed co-localization of lesions and central veins

GEPCI not only provided images that were similar to those obtained with standard images (Figure 1), but also provided additional contrasts beyond what is seen using standard clinical sequences. GEPCI T1f delineated GM and WM (Figure 1). GEPCI provided susceptibility weighted images (SWI) that revealed venous structures in the brain. Other investigator groups have used the combination of FLAIR images and SWI contrast images to demonstrate veins localized within white matter¹⁵ and MS lesions.¹⁶⁻¹⁹ The latter has required careful co-registration of separate FLAIR and SWI images. GEPCI - T2*-SWI provided simultaneous co-registered visualization of MS lesions and veins, thus avoiding potential problems with image registration when combining separate images. We therefore used GEPCI-T2*-SWI (Figure 2) to enumerate lesions that were visibly associated with

central veins in the RRMS group, where distinct lesions were readily identifiable. Among a total of 139 lesions, 106 (76%) had a vein within the lesion, 13 (9.3%) of which had multiple veins. Thirty-three (24%) lesions did not show obvious internal veins. The prevalence of discernible co-localization of lesions and veins was similar among each of our RRMS subjects, ranging from 66.7% to 84.6%.

Discussion

This study of thirty MS subjects representing a range of clinical subtypes and disability levels used GEPCI to quantitatively evaluate MS white matter tissue integrity. The MSFC was used to produce both separate and composite quantitative clinical scores to examine the relationship between MRI and clinical measurements. Based on the strength of correlations, GEPCI proved better than conventional MRI. The strongest correlation observed was between GEPCI-TDL and MSFC 2'' (Spearman $\rho = -0.644$), which includes a sensitive measure of cognition (PASAT 2''). TDL, a measure that incorporates lesion severity as well as size, performed consistently better than LL-GEPCI or standard LL-FLAIR. Incorporation of lesion severity as well as volume improved the correlations, supporting the utility of GEPCI quantitative relaxometry maps.

Correlations between GEPCI-based TDL and LL and the composite MSFC were stronger than correlations with the individual component scores of the MSFC (Spearman ρ -0.458, -0.461 and -0.454 respectively). This suggested that these correlations were not entirely driven by any single component of MSFC. This same statement regarding composite vs. individual score correlations was also true for FLAIR based lesion load assessment (LL-FLAIR). However, the stronger correlation between MSFC 2'' and TDL-GEPCI versus LL-FLAIR was driven by the PASAT 2'' component.

GEPCI correctly distinguished the pre-defined MS clinical subtypes in 70% of all subjects, with $R2^*$ distribution width ($R2^*_{(w)}$) and TDL being the major distinguishing criteria. Of note, the $R2^*_{(w)}$ and the $R2^*$ center ($R2^*_{(c)}$) characterizing the semi-Gaussian distribution of MS brain $R2^*$ relaxation rate parameters did not demonstrate significant correlation with clinical disability tests, yet provided additional information for clinical subtype classification. In particular, an increased $R2^*_{(w)}$ was important for distinguishing RRMS from SPMS. A larger $R2^*_{(w)}$ extending the distribution function toward lower $R2^*$ values likely reflects damage in the NAWM, which is difficult to discern by conventional MRI.²⁰ Considering that MS subtypes are determined based on clinical and disease course,²¹ which includes disability evolution through time, whereas MR measures the brain tissue at a single time-point, this 70% level of agreement supports the ability of GEPCI to capture the underlying pathological differences between different disease courses. This capability might be especially useful in evaluations of new treatments, and thus studies with larger sample sizes are planned to confirm our observations.

Neither TDL-GEPCI nor LL (by either GEPCI or standard FLAIR) correlated significantly with EDSS, which is often considered to be the 'gold standard' clinical measure of MS disability. In our study EDSS correlated poorly with all cognitive tests: PASAT 3'' ($\rho = -0.42$), PASAT 2'' ($\rho = -0.36$) and SDMT ($\rho = -0.36$), while it correlated strongly with

25' walk ($\rho = -0.87$). This result is in accord with the fact that EDSS is weighted toward capturing lower limb dysfunction, which is reflected in the 25'-walk component of the MSFC.²² Walking dysfunction in MS can often be attributed to spinal cord lesions, which were not imaged in this study.

The T2*-SWI images allowed precise co-localization of veins and MS lesions, without lengthening the imaging protocol. The relationship of veins to MS lesions during lesion development is of great interest, and might provide insights into MS pathogenesis. A reduction of periventricular venous density with growing disease severity as well as an increase in venous proportion in newly developed plaques have been observed.^{23, 24} We also observed a trend of less visible veins in lesions with increasing disability among RRMS patients. More insights could be provided with larger group of subjects and follow up studies.

A few limitations of the present study should be taken into account while interpreting its findings. The sample sizes are small. Subjects from each of the MS clinical subtypes may not be entirely representative of their subtype. We recruited subjects from the MS clinic in a semi-random fashion, enrolling patients whose clinical subtype was unequivocal, while also trying to have a range of EDSS scores that was overlapping between subgroups. The SPMS subgroup had longer disease duration than either of the other two subgroups and this may have influenced parameters contributing to the ability of GEPCI to discriminate subgroups. Moreover, in our MRI assessment, we focused on analyses of cerebral WM, without taking into account other important regions such as deep gray matter structures, cerebral cortex, or the limbic system. In this regard, it should be noted that for our comparative analyses we matched the scope of the conventional FLAIR images to GEPCI, and GEPCI proved to be better. Additionally, the parameter R2* might be affected by factors beyond MS. For example, R2* is known to increase with iron accumulation in deep GM which happens with aging²⁵ and in MS²⁶. On the other hand, decreased iron deposition in WM²⁷ would decrease R2*, and thereby widen the R2* distribution and contribute to changes in R2*_(w) and R2*_(c) of the semi-Gaussian curve. Also, while we expected R2* to decrease with neuronal tissue loss (more water in the tissue), the MS brain also undergoes accelerated volume loss, which may counteract the dropping macromolecule concentration in tissue. Field inhomogeneity is also known to affect R2* values, which led us to exclude regions that are sensitive to this artifact in our current analysis.

We have herein demonstrated several benefits of GEPCI for clinical and research applications. Additionally, GEPCI is time efficient: 6 min 26 sec for GEPCI versus a total of 15 min scan time for T1W, T2W and FLAIR images using standard clinical protocol, and it can be used safely in high-field MRI because it is based on gradient echo MRI and uses small flip angles as compared with spin-echo based techniques, thus eliminating energy deposition problems. Although it remains a huge challenge to relate clinical manifestations to brain tissue damage quantitated using imaging, compared with standard MRI scans GEPCI represents a step toward enhancing correlations between clinical and radiological measures. Improved imaging methods that better reflect the underlying disease process will aid in the treatment of individuals with MS, as well as expedite evaluations of proposed new treatments. Further studies using GEPCI of larger MS populations with longitudinal follow-

ups are needed to determine a role that GEPCI can play in the evaluation of new therapeutics.

Supplementary Material

Refer to Web version on PubMed Central for supplementary material.

Acknowledgments

We thank the patient participants, and the clinicians who referred them to this study, Drs. Becky Jo Parks, Robert T. Naismith, Gregory Wu, Eric Klawiter and Enrique Alvarez. We thank Susan Fox and Nhial Tutlam for assistance in coordinating the study.

Funding

The study was funded by the Department of Defense of the United States [grant MS090031]; and the National Institute of Health grants [CO6 RR020092, UL1 TR000448] (Washington University Institute of Clinical and Translational Sciences - Brain, Behavioral and Performance Unit); AHC was supported in part by The Manny and Rosalyn Rosenthal-Dr. John L. Trotter MS Center Chair in Neuroimmunology from the Barnes-Jewish Hospital Foundation.

References

1. Mainero C, De Stefano N, Iannucci G, et al. Correlates of MS disability assessed in vivo using aggregates of MR quantities. *Neurology*. 2001; 56:1331–1334. [PubMed: 11376183]
2. Li DKB, Held U, Petkau J, et al. MRI T2 lesion burden in multiple sclerosis - A plateauing relationship with clinical disability. *Neurology*. 2006; 66:1384–1389. [PubMed: 16682671]
3. Sormani MP, Rovaris M, Comi G, Filippi M. A reassessment of the plateauing relationship between T2 lesion load and disability in MS. *Neurology*. 2009; 73:1538–1542. [PubMed: 19794123]
4. Barkhof F. The clinico-radiological paradox in multiple sclerosis revisited. *Curr Opin Neurol*. 2002; 15:239–245. [PubMed: 12045719]
5. Papanikolaou N, Papadaki E, Karampekios S, et al. T2 relaxation time analysis in patients with multiple sclerosis: correlation with magnetization transfer ratio. *European Radiology*. 2004; 14:115–122. [PubMed: 14600774]
6. Seewann A, Vrenken H, van der Valk P, et al. Diffusely Abnormal White Matter in Chronic Multiple Sclerosis Imaging and Histopathologic Analysis. *Archives of Neurology*. 2009; 66:601–609. [PubMed: 19433660]
7. Sormani MP, Bruzzi P, Beckmann K, et al. MRI metrics as surrogate endpoints for EDSS progression in SPMS patients treated with IFN beta-1b. *Neurology*. 2003; 60:1462–1466. [PubMed: 12743232]
8. van Walderveen MAA, Lycklama a Nijeholt GJ, Ader HJ, et al. Hypointense lesions on T1-weighted spin-echo magnetic resonance imaging - Relation to clinical characteristics in subgroups of patients with multiple sclerosis. *Archives of Neurology*. 2001; 58:76–81. [PubMed: 11176939]
9. Luo J, Jagadeesan BD, Cross AH, Yablonskiy DA. Gradient Echo Plural Contrast Imaging - Signal model and derived contrasts: T2*, T1, Phase, SWI, T1f, FST2* and T2*-SWI. *Neuroimage*. 2012; 60:1073–1082. [PubMed: 22305993]
10. Sati P, Cross AH, Luo J, Hildebolt CF, Yablonskiy DA. In vivo quantitative evaluation of brain tissue damage in multiple sclerosis using gradient echo plural contrast imaging technique. *Neuroimage*. 2010; 51:1089–1097. [PubMed: 20338247]
11. Gaitan MI, de Alwis MP, Sati P, Nair G, Reich DS. Multiple sclerosis shrinks intralésional, and enlarges extralésional, brain parenchymal veins. *Neurology*. 2013; 80:145–151. [PubMed: 23255828]
12. Kurtzke JF. Rating Neurologic Impairment in Multiple-Sclerosis - an Expanded Disability Status Scale (Edss). *Neurology*. 1983; 33:1444–1452. [PubMed: 6685237]

13. Cohen JA, Reingold SC, Polman CH, Wolinsky JS. Disability outcome measures in multiple sclerosis clinical trials: current status and future prospects. *Lancet Neurology*. 2012; 11:467–476.
14. *Modeling and Multivariate Methods*. Cary, North Carolina: SAS Institute Inc.; 2012. JMP®10.
15. Reichenbach JR, Venkatesan R, Schillinger DJ, Kido DK, Haacke EM. Small vessels in the human brain: MR venography with deoxyhemoglobin as an intrinsic contrast agent. *Radiology*. 1997; 204:272–277. [PubMed: 9205259]
16. Sati P, George IC, Shea CD, Gaitan MI, Reich DS. FLAIR*: A Combined MR Contrast Technique for Visualizing White Matter Lesions and Parenchymal Veins. *Radiology*. 2012
17. Tallantyre EC, Brookes MJ, Dixon JE, Morgan PS, Evangelou N, Morris PG. Demonstrating the perivascular distribution of MS lesions in vivo with 7-Tesla MRI. *Neurology*. 2008; 70:2076–2078. [PubMed: 18505982]
18. Tallantyre EC, Dixon JE, Donaldson I, et al. Ultra-high-field imaging distinguishes MS lesions from asymptomatic white matter lesions. *Neurology*. 2011; 76:534–539. [PubMed: 21300968]
19. Grabner G, Dal-Bianco A, Scherthaner M, Vass K, Lassmann H, Trattnig S. Analysis of Multiple Sclerosis Lesions Using a Fusion of 3.0 T FLAIR and 7.0 T SWI Phase: FLAIR SWI. *J Magn Reson Imaging*. 2011; 33:543–549. [PubMed: 21563237]
20. Fisher E, Chang A, Fox RJ, et al. Imaging correlates of axonal swelling in chronic multiple sclerosis brains. *Annals of Neurology*. 2007; 62:219–228. [PubMed: 17427920]
21. Lublin FD, Reingold SC. Defining the clinical course of multiple sclerosis: Results of an international survey. *Neurology*. 1996; 46:907–911. [PubMed: 8780061]
22. Rudick RA, Cutter G, Reingold S. The multiple sclerosis functional composite: a new clinical outcome measure for multiple sclerosis trials. *Mult Scler*. 2002; 8:359–365. [PubMed: 12356200]
23. Sinnecker T, Bozin I, Dorr J, et al. Periventricular venous density in multiple sclerosis is inversely associated with T2 lesion count: a 7 Tesla MRI study. *Mult Scler J*. 2013; 19:316–325.
24. Dal-Bianco, A.; Grabner, G.; Lassmann, H., et al. Proceedings of International Society for Magnetic Resonance in Medicine. Utah: 2013. A 7-Tesla Longitudinal Study on Proportion of Veins in Plaques of Patients with Multiple Sclerosis; p. 0163
25. Hallgren B, Sourander P. The Effect of Age on the Non-Haemin Iron in the Human Brain. *Journal of Neurochemistry*. 1958; 3:41–51. [PubMed: 13611557]
26. Duyn JH. High-field MRI of brain iron. *Methods Mol Biol*. 2011; 711:239–249. [PubMed: 21279605]
27. Paling D, Tozer D, Wheeler-Kingshott C, Kapoor R, Miller DH, Golay X. Reduced R2' in multiple sclerosis normal appearing white matter and lesions may reflect decreased myelin and iron content. *J Neurol Neurosurg Psychiatry*. 2012; 83:785–792. [PubMed: 22626944]

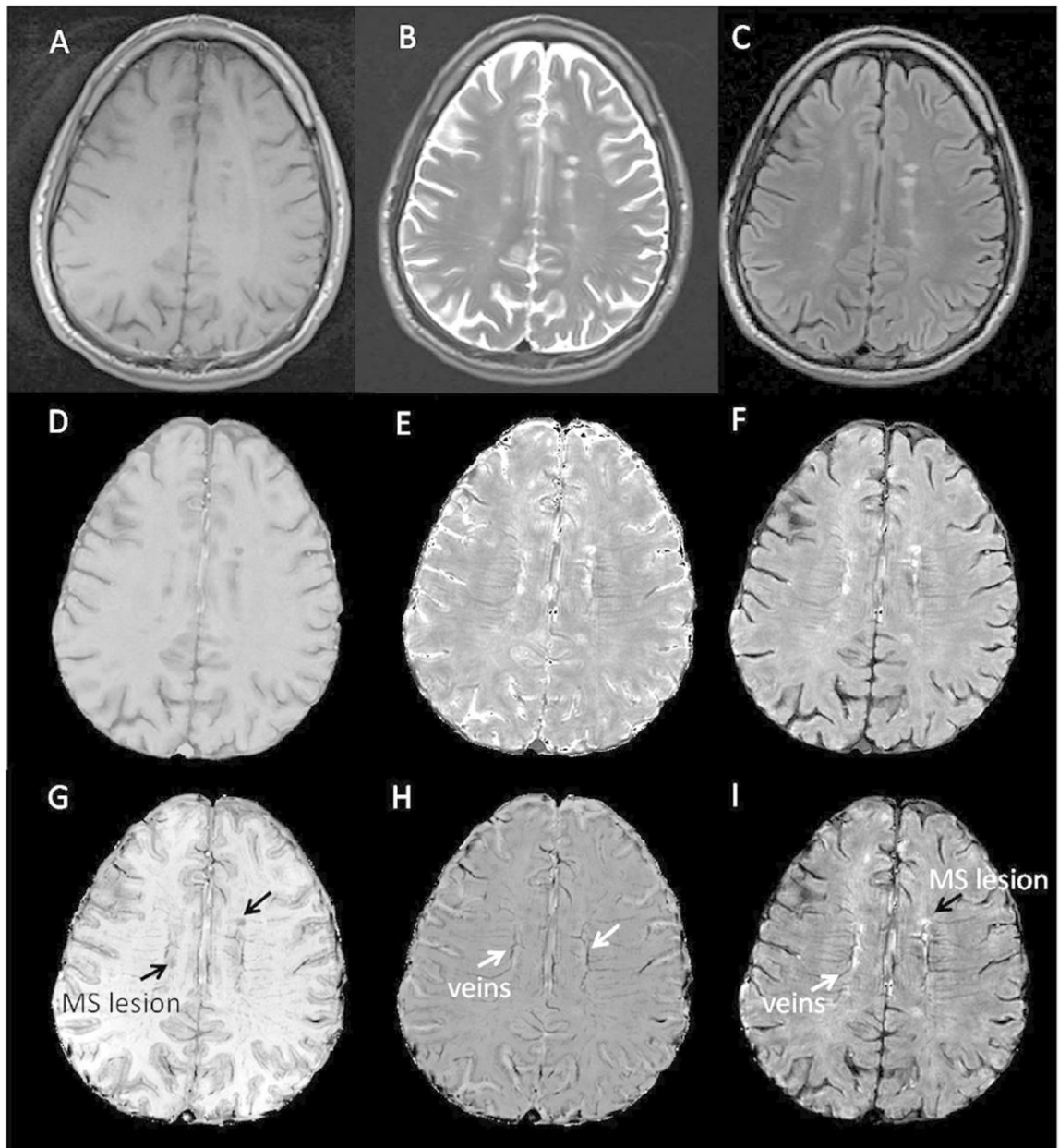


Figure 1.

Standard clinical images for MS compared to GEPCI images.

Top row shows standard images: A: T1W, B: T2W, and C: FLAIR. Second row shows GEPCI images that match clinical images: D: GEPCI-T1W, E: GEPCI-T2* map, F: GEPCI-FST2*. Bottom row shows additional GEPCI contrasts: G: T1f, H: GEPCI-SWI, I: T2*-SWI.

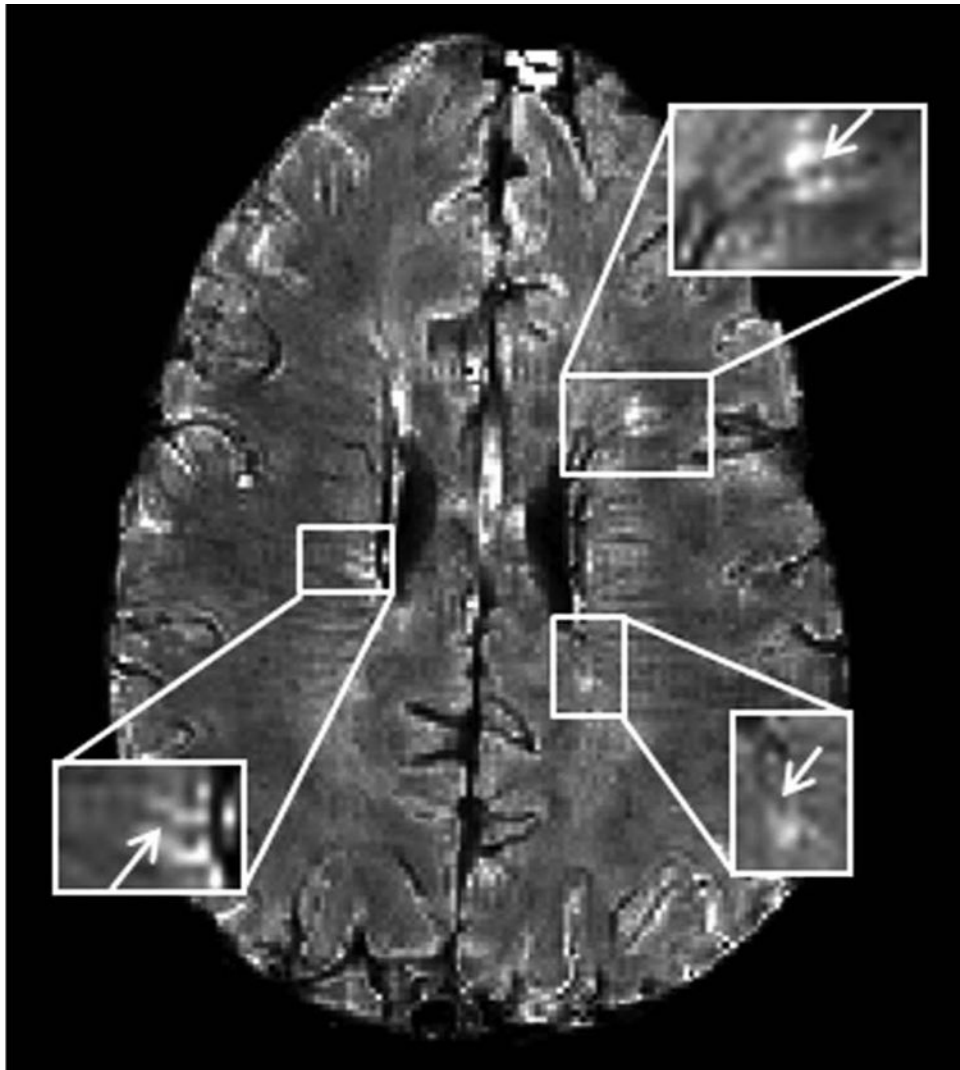


Figure 2. Co-localization of MS lesions with veins using GEPCI. T2*-SWI image ($1 \times 1 \times 3 \text{ mm}^3$ resolution) in a 33-year-old man with relapsing-remitting MS (EDSS = 4.0, disease duration = 14 years). Three lesions with central veins (arrows) are depicted.

Table 1

Baseline demographics

Characteristics	Values			
	overall	RRMS	PPMS	SPMS
No.	30	10	10	10
Age, y. median (range)	51.5 (27 to 70)	44 (27 to 52)	54.5 (40 to 70)	52.5 (41 to 64)
Gender, F:M	16:14	6:4	6:4	4:6
EDSS, median (range)	5.5 (1.5 to 8.0)	2.5 (1.5 to 6.5)	5.75 (3.5 to 8.0)	6.0 (4.0 to 6.5)
Disease Duration, y.	13 (3 to 34)	7 (3 to 14)	9 (4 to 26)	25.5 (17 to 34)

Author Manuscript

Author Manuscript

Author Manuscript

Author Manuscript

Table 2

Correlations between clinical and radiological measurements for all subjects.

	EDSS	MSFC 3 ^a	PASAT 3 ^a	MSFC 2 ^a	PASAT 2 ^a	25' Walk	9-HPT	SDMT
TDL	0.343	-0.524 ***	-0.314	-0.644 *****	-0.458 *	-0.461 *	-0.454 *	-0.444 *
LL-GEPCI	0.311	-0.500 **	-0.292	-0.630 *****	-0.447 *	-0.458 *	-0.402 *	-0.429 *
R²*(w)	0.127	-0.074	-0.083	-0.146	-0.130	-0.066	-0.166	-0.141
R²*(c)	-0.017	0.088	-0.038	0.057	0.004	0.088	0.120	0.073
LL-FLAIR	0.348	-0.455 *	-0.254	-0.544 *****	-0.307	-0.405 *	-0.461 *	-0.423 *

Spearman ρ between GEPCI scores, FLAIR and Clinical measurements of disability.

p: Probability > |p|;

* p<0.05,

** p<0.01,

*** p<0.005,

***** p<0.001.